

Entangled microwaves from quantum dots

C. Emery, B. Trauzettel, and C. W. J. Beenakker

Instituut-Lorentz, Universiteit Leiden, P.O. Box 9506, 2300 RA Leiden, The Netherlands

(Dated: February 23rd, 2005)

We describe a mechanism for the production of polarisation-entangled microwaves using intra-band transitions in a pair of quantum dots. This proposal relies neither on spin-orbit coupling nor on control over electron-electron interactions. The quantum correlation of microwave polarisations is obtained from orbital degrees of freedom in an external magnetic field. We calculate the concurrence of emitted microwave photon pairs, and show that a maximally entangled Bell pair is obtained in the limit of weak inter-dot coupling.

PACS numbers: 42.65.Lm, 78.67.Hc, 78.70.Gq

Entangled photons at optical frequencies are routinely produced by non-linear optical effects in macroscopic crystals [1]. The use of semiconductor nanostructures to produce these states promises both a greater frequency range and a closer integration with quantum electronics.

One way to produce entangled photons is to start with entangled electrons and then transfer this entanglement [2]. However, one can also start with non-entangled particles, and most work in this area has focused on the decay of bi-excitonic states in quantum dots [3, 4, 5, 6]. In the original proposal [3], a bi-exciton is formed in a single dot by electrical pumping, and then subsequently decays by emitting a pair of photons via one of two cascades. The polarisations of these two photons are linked to the cascade by which the bi-exciton decays, and thus, if these cascades proceed coherently, one produces polarisation-entangled photons. All these proposals [2, 3, 4, 5, 6] involve *inter*-band transitions between valence and conduction bands of a quantum dot, so that the output photons have frequencies in the *visible* range.

In this paper, we propose the use of *intra*-band transitions of conduction band electrons to generate entangled *microwave* photons. Our proposal, illustrated in Fig. 1, can be seen as the real-space analogue of the bi-exciton decay cascade in energy of Ref. [3]. The microwaves originate from spontaneous downward transitions between single-particle levels in a quantum dot. That these transitions couple to microwaves has been demonstrated in photon-assisted tunnelling experiments [7].

Experiments on phonon emission [8] have shown that the intra-band transitions are subject to selection rules. We argue that selection rules also apply to the emission of electromagnetic radiation and that they determine not only the possibility of a transition occurring, but also the polarisation of the emitted radiation. For a quantum dot with cylindrical symmetry, conservation of angular momentum requires that emitted microwaves be circularly polarised (CP) in the plane of the dot. We show later that the dots can be designed to produce predominantly one of two circular polarisations, which we denote CP+ and CP-, with the same frequency Ω .

Our entanglement scheme requires four quantum dots

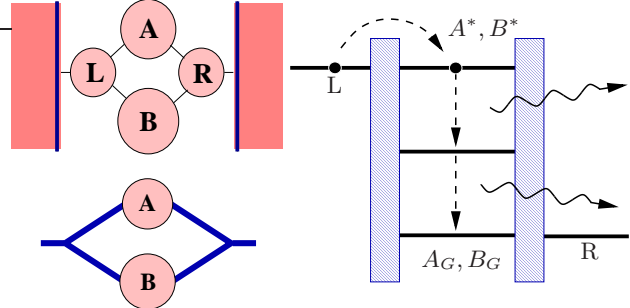


FIG. 1: Schematic of the microwave entangler. Upper left: The four dot arrangement between two electron reservoirs. Lower left: Alternative arrangement with two dots and two Y-junctions. Right panel: Positions of dot levels in the four dot configuration. An electron tunnels through the single level in dot L into a superposition $\alpha|A^*\rangle + \beta|B^*\rangle$ of upper levels in dots A and B . It decays to the ground state with the emission of two photons. The resulting state $\alpha|A_G\rangle|++\rangle + \beta|B_G\rangle|--\rangle$ encodes the state of the quantum dot onto pairs of photons with left (CP+) or right (CP-) circular polarisation. Subsequent tunnelling of the electron out of the lower levels into dot R establishes a unique final state for the electron, thus separating the dot-field wave function and liberating the entangled microwave pair.

as shown in Fig. 1: two dots (L, R) to provide unique initial and final states for the electron, and two more dots (A, B) to provide the two decay paths. An alternative scheme, in which the dots L and R are replaced by Y-junctions, is discussed briefly at the end of the paper. Tunnelling of an electron into the upper level of dot A is followed by the spontaneous emission of two CP+ microwave photons as the electron decays to its ground state. Dot B is configured such that the same process in it gives rise to two CP- photons (we will describe later how this can be done). The classical correlation between the polarisations of the two photons (both CP+ or both CP-) becomes a quantum entanglement because of phase coherence of the two paths $L \rightarrow A \rightarrow R$ and $L \rightarrow B \rightarrow R$.

Whilst not strictly necessary for the entangling mech-

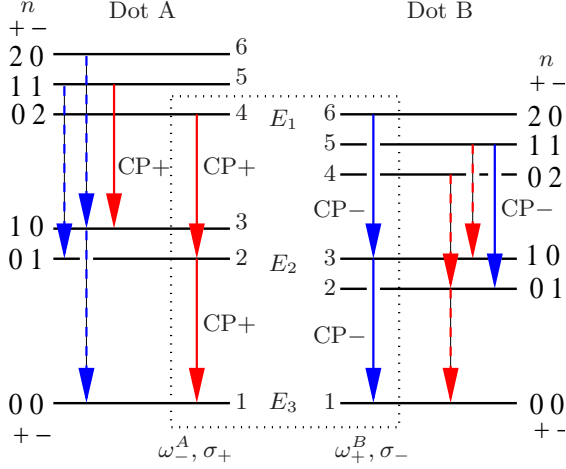


FIG. 2: Fock-Darwin spectrum of dots A and B : the six lowest levels with their quantum numbers n_{\pm} are shown for each dot. The dot sizes are tuned such that $\omega_{-}^A = \omega_{+}^B = \Omega$. Selection rule allowed transitions are shown, with solid (dashed) arrows denoting on (off) resonant transitions. The circular polarisation, $CP+$ or $CP-$, of the emitted microwaves is also shown. In the entangler, electrons are injected into the two levels at E_1 , and decay via the transitions shown in the dotted rectangle. In dot A , this produces a cascade of two $CP+$ photons, whereas in dot B two $CP-$ photons are produced.

anism, it is helpful to assume that the quantum dots are inserted into a cylindrical microwave resonator able to support both polarisations at the resonant frequency Ω . Recent results for double quantum dots and superconducting transmission line resonators have shown the possibility of extremely large dot-microwave couplings [9, 10]. The cavity ensures that microwave, and not phonon, transitions dominate, and also serves to counteract any slight non-idealities in the quantum dot emission frequencies that might otherwise render the two decay paths distinguishable. The resultant entanglement could be detected via the violation of a Bell inequality. This is a routine experiment for visible light; the analogous experiment at microwave frequencies is an experimental challenge, with some recent progress [11].

We begin our more detailed treatment by describing the circularly polarised microwave transitions. The two emitting quantum dots, A and B , are assumed to have cylindrically symmetric, parabolic confining potentials. To avoid complication from the spin degree of freedom, which plays no role here, we take a large in-plane magnetic field to spin polarise the electrons. A small perpendicular field B_0 is added to control the microwave polarisations, as we discuss shortly.

Since we never occupy the dots with more than one electron at a time, a single-particle picture is appropriate (no Kondo effect is possible because of the spin polarisation). The Hamiltonian of quantum dot $Y = A, B$

is

$$H_Y = \omega_{+}^Y a_{+}^{Y\dagger} a_{+}^Y + \omega_{-}^Y a_{-}^{Y\dagger} a_{-}^Y = \sum_i \varepsilon_i^Y |Y_i\rangle \langle Y_i|. \quad (1)$$

The excitation energies are $\omega_{\pm}^Y = \sqrt{\omega_0^Y{}^2 + \omega_c^2/4} \pm \omega_c/2$, with $\omega_c = eB_0/m$ the cyclotron frequency and ω_0^Y the confinement energy of dot Y (we set $\hbar = 1$). This so-called Fock-Darwin spectrum [12] is thus determined by the two quantum numbers n_{\pm}^Y .

The intensity of electric dipole transitions between dot levels is proportional to $|\mathbf{d}|^2$, where \mathbf{d} is the matrix element of the position operator \mathbf{r} between the initial and final states. The operator $\sigma^{\pm} = x \pm iy$ produces a $CP\pm$ electric field in the $x-y$ plane of the dot. In terms of the raising and lowering operators a_{\pm}^{\dagger} and a_{\pm} , we have $\sigma^{\pm} = \tilde{l}(a_{\pm}^{\dagger} + a_{\mp})$ with $\tilde{l} = [m^2(\omega_0^2 + \omega_c^2/4)]^{-1/4}$. The electric dipole transitions thus have the selection rule $|\Delta n_{\pm}| = 1$. Transitions in which n_{-} decreases emit $CP+$ photons, and transitions in which n_{+} decreases emit $CP-$ photons.

Figure 2 shows the six lowest levels $|Y_i\rangle$ in dots $Y = A, B$, labelled $i = 1$ to 6 from the bottom up. We take B_0 small enough that there are no level crossings in the spectrum. Since ω_{\pm} depends on the confinement energy ω_0 , the spectra of the dots can be tuned by electrostatically changing their sizes. We set ω_{-} of dot A equal to ω_{+} of dot B by choosing the ratio of the linear sizes to be $l_A/l_B \approx 1 - l_B^2/2l_c^2$ for $l_c \gg l_B$, with $l_c = \sqrt{\hbar/eB_0}$ the magnetic length. Fixing $\omega_{-}^A = \omega_{+}^B = \Omega$, only one free parameter $\omega_c \ll \Omega$ remains to specify the two spectra.

Dots A and B are in tunnelling contact with the single levels in dots L and R . The state E_L of dot L is aligned with the levels E_1 in dots A and B , and the single level E_R in dot R is aligned with the ground states at E_3 . The chemical potentials of the electron reservoirs are adjusted such that on the left $\mu_L \gg E_L$ and on the right $\mu_R \ll E_R$. The dots are set in a small area such that the charging energy is sufficient to prevent more than one electron being in the four-dot system at any one time.

We calculate the coupled dynamics of electron and photons from the master equation [13, 14, 15],

$$\frac{d}{dt}\rho = -i[H, \rho] + \mathcal{L}[\rho]. \quad (2)$$

The commutator describes the coherent evolution of the density matrix ρ under the action of the Hamiltonian H of the dot-cavity system. The operator $\mathcal{L}[\rho]$ describes the effects of coupling of the dot R to the electron reservoir on the right. As we are interested in the entanglement produced by the passage of a single electron through the device, we initialise the system with an electron in dot L . The left reservoir serves only to populate this level initially and is then decoupled, while the coupling to the right reservoir is permanent and acts as a sink for the electron.

The Hamiltonian is $H = \sum_Y H_Y + H_T + H_+ + H_- + H_\mu$, with the sum Y taken over all four dots. The Hamiltonians of the dots A and B contain six levels each, according to Eq. (1). For dots L and R we have $H_L = E_L|L\rangle\langle L|$ and $H_R = E_R|R\rangle\langle R|$. We set $E_L = E_1$ and $E_R = E_3$. The dots are connected via the tunnelling Hamiltonian

$$H_T = \sum_{i=1}^6 \{ T_{LA_i} |L\rangle\langle A_i| + T_{RA_i} |R\rangle\langle A_i| + T_{LB_i} |L\rangle\langle B_i| + T_{RB_i} |R\rangle\langle B_i| \} + \text{h.c.}, \quad (3)$$

where T_{XY_i} are tunnel amplitudes.

The microwave photons have the Hamiltonians $H_+ = \omega_-^A b_+^\dagger b_+$ and $H_- = \omega_+^B b_-^\dagger b_-$, with b_\pm the field operators of CP \pm microwaves. Since we are on resonance, $\omega_-^A = \omega_+^B = \Omega$. In the rotating wave approximation, the emission of microwaves is governed by the Hamiltonian

$$H_\mu = g^A \{ |A_5\rangle\langle A_3| + |A_4\rangle\langle A_2| + |A_2\rangle\langle A_1| \} b_+^\dagger + g^B \{ |B_6\rangle\langle B_3| + |B_5\rangle\langle B_2| + |B_3\rangle\langle B_1| \} b_-^\dagger + \text{h.c.}, \quad (4)$$

neglecting off-resonant transitions.

The coupling of the right electron reservoir to dot R is incorporated into the master equation through the Lindblad operator $\mathcal{L}[\rho] = D\rho D^\dagger - \frac{1}{2}D^\dagger D\rho - \frac{1}{2}\rho D^\dagger D$. The jump operator is $D = \sqrt{\Gamma_R} |0_{\text{dot}}\rangle\langle R|$, with Γ_R the tunnelling rate and $|0_{\text{dot}}\rangle$ denoting all four dots empty. In the following, we will for simplicity set $g^A = g^B = g$ and $T_{XA_i} = T_A$, $T_{XB_i} = T_B$ for $X = L, R$ and $i = 1, \dots, 6$.

We work in a weak coupling limit, not only for the inter-dot couplings $T_A, T_B \ll \Omega$, but also for the dot-field coupling $g \ll \Omega$. This allows us to truncate the Hilbert space to include only the following states: For the uppermost three electronic states in dots A and B , and for the state in the left dot, we keep only empty field states. For the middle two states in A and B , we keep states with zero or one photons. For the ground states of A and B , for the state in dot R , and for the empty dot, we retain states of 0, 1, and 2 photons. Furthermore, we only couple CP $+$ photons to an electron in dot A , and CP $-$ photons to an electron in dot B . Results of a numerical integration of the master equation (2) are plotted in Figs. 3 and 4.

The density matrix of the field is obtained by tracing out the dot degrees of freedom from the density matrix $\rho(t)$. We denote its (unnormalised) two-photon projection as $\chi(t)$. It has the form

$$\chi = r_+ |++\rangle\langle ++| + r_- |--\rangle\langle --| + r_c |+-\rangle\langle -+| + r_c^* |-+\rangle\langle +-. \quad (5)$$

The mean number of photon pairs in the cavity is given by $N_2 = \text{Tr } \chi = r_+ + r_-$. This is plotted as a function of time in Fig. 3. The time scale on which the electron is transmitted sequentially through the elements of the

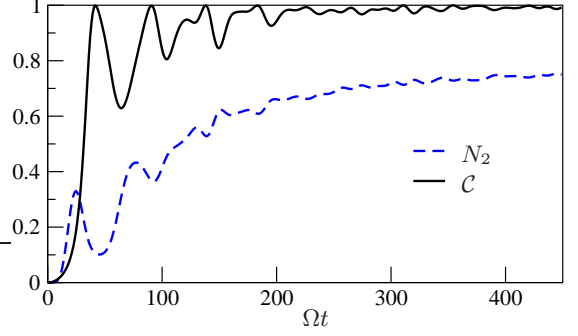


FIG. 3: Dynamics of the microwave entangler. Plotted is the time-dependence of the mean number of photon pairs in the cavity N_2 and their degree of entanglement \mathcal{C} (the concurrence). For long times, the field approaches a steady state with, for the weak coupling $T_A = T_B = 0.05 \Omega$ shown here, a high proportion of photon pairs $N_2^\infty \approx 0.7$ and almost maximal concurrence $\mathcal{C}^\infty \approx 1$. Model parameters were $\omega_c = g = \Gamma_R = 0.1 \Omega$.

system is $\tau = \Gamma_R^{-1} + 2g^{-1} + T_A^{-1} + T_B^{-1}$. We see that for times $t \gg \tau \approx 70 \Omega^{-1}$, the number of photon pairs N_2 approaches a stationary value, N_2^∞ .

The degree of entanglement (concurrence) \mathcal{C} of the photon pair can be calculated using Wootter's formula [16] for the concurrence of the density matrix $\chi(t)$, which in general describes a mixed state. We find

$$\mathcal{C} = \frac{2|r_c|}{r_+ + r_-}. \quad (6)$$

The time-dependent concurrence $\mathcal{C}(t)$ is shown in Fig. 3, and this is also seen to saturate for $t \gg \tau$. In Fig. 4 (upper panel) we plot this long-time limit \mathcal{C}^∞ as a function of the coupling asymmetry T_A/T_B for several values of T_A .

An analytical solution is possible for $T_A, T_B \ll \omega_c$. Since the top three levels in dots A and B are each separated by ω_c , when $T_A, T_B \ll \omega_c$ the electron tunnels from dot L only into the resonant levels at E_1 , producing a photon-pair before leaving the dots. In this limit, the concurrence \mathcal{C}^∞ of the final state is easily calculated, as the relative amplitudes for the generation of each of the two photon pairs are proportional to the product of the individual coupling amplitudes along each of the two paths. We find

$$\mathcal{C} = 2 \frac{|T_A T_B g_A g_B|^2}{|T_A g_A|^4 + |T_B g_B|^4}. \quad (7)$$

The numerical weak coupling results in Fig. 4 (crosses), are very close to this analytic result (solid curve). For weak, symmetric inter-dot couplings, the concurrence approaches unity, corresponding to the production of the Bell state $2^{-1/2}(|++\rangle + |--\rangle)$.

Successful operation of the device requires that, after the passage of the electron, the cavity is left with a pair

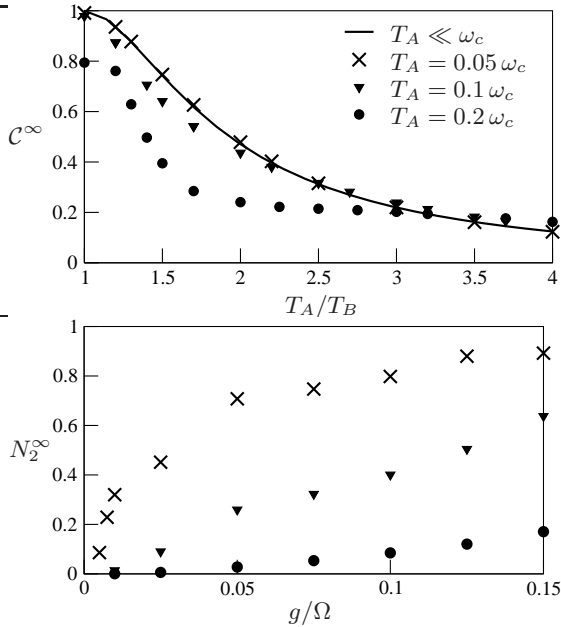


FIG. 4: Performance of the microwave entangler. Upper panel: The asymptotic entanglement of the photon pairs as a function of the asymmetry in the couplings of dots A and B to the other two dots. The solid curve is the analytic result (7) for $T_A, T_B \ll \omega_c$. We fixed $g = \omega_c$. Lower panel: Probability N_2^∞ of successful operation of the entangler as a function of the dot-microwave coupling g . The symbols correspond to the same values of T_A as in the upper panel and we fixed $T_A = T_B$. In both plots we took $\omega_c = \Gamma_R = 0.1 \Omega$.

of microwave photons. The probability of successful operation is thus given by the asymptotic mean number of photon pairs N_2^∞ . This probability is plotted in Fig. 4 (lower panel). Smaller inter-dot couplings give rise to a higher success probability.

The model can be extended to include direct inelastic transitions from upper levels in dots A and B into dot R . This reduces the number of photon pairs produced, but provided that the rate of these inelastic processes is smaller than the dot-cavity coupling, photon-pair production will still dominate. Moreover, provided that these inelastic processes give no which-way information on the path of the electron, affecting the two dots roughly equally, they have little effect on the degree of entanglement of the photon pairs that are emitted.

In principle the microwave entangler could be constructed using only two dots, with dots L and R being replaced by Y-junctions (Fig. 1, lower left). The condition for this arrangement to work is that the two dots are connected to within a Fermi wavelength of each other at

the Y-junctions. This ensures that an electron tunnels coherently into both dots [17].

In summary, we have described a mechanism for the production of entangled microwave photon pairs using intra-band transitions in a quantum dot. Our calculations indicate that a four-dot device is capable of the output of highly entangled pairs with reasonable success probability. The entangler may be thought of as an electron interferometer in which each of the two paths is coupled to a different photon-pair producing process. Apart from the different frequency range, it differs from the celebrated bi-exciton entangler [3] in that the two interfering paths are in real space, rather than in energy space, and also in that the correlated polarisations result from orbital selection rules — rather than from spin-orbit coupling.

This work was supported by the Dutch Science Foundation NWO/FOM.

- [1] L. Mandel and E. Wolf, *Optical Coherence and Quantum Optics* (Cambridge, 1995).
- [2] V. Cerletti, O. Gywat, and D. Loss, cond-mat/0411235.
- [3] O. Benson, C. Santori, M. Pelton, and Y. Yamamoto, Phys. Rev. Lett. **84**, 2513 (2000).
- [4] O. Gywat, G. Burkard, and D. Loss, Phys. Rev. B **65**, 205329 (2002).
- [5] T. M. Stace, G. J. Milburn, and C. H. W. Barnes, Phys. Rev. B **67**, 085317 (2003).
- [6] J. I. Perea and C. Tejedor, cond-mat/0409745.
- [7] W.G. van der Wiel, S. de Franceschi, J. M. Elzerman, T. Fujisawa, S. Tarucha, and L. P. Kouwenhoven, Rev. Mod. Phys. **75**, 1 (2003).
- [8] T. Fujisawa, D. G. Austing, Y. Tokura, Y. Hirayama, and S. Tarucha, Nature **419**, 278 (2002).
- [9] A. Blais, R.-S. Huang, A. Wallraff, S. M. Girvin, and R. J. Schoelkopf, Phys. Rev. A **69**, 062320 (2004).
- [10] L. Childress, A. S. Sørensen, and M. D. Lukin, Phys. Rev. A **69**, 042302 (2004).
- [11] J. Gabelli, L.-H. Reydellet, G. Fèvre, J.-M. Berroir, B. Plaçais, P. Roche, and D. C. Glattli, Phys. Rev. Lett. **93**, 056801 (2004).
- [12] L. P. Kouwenhoven, D. G. Austing, and S. Tarucha, Rep. Prog. Phys. **64**, 701 (2001).
- [13] T. H. Stoof and Yu. V. Nazarov, Phys. Rev. B **53**, 1050 (1996).
- [14] S. A. Gurvitz, Phys. Rev. B **57**, 6602 (1998).
- [15] T. Brandes, cond-mat/0409771.
- [16] W. K. Wootters, Phys. Rev. Lett. **80**, 2245 (1998).
- [17] F. Marquardt and C. Bruder, Phys. Rev. B **68**, 195305 (2003).